2015

Visualization Techniques of Shear Wave Propagation in Wormlike Micellar Fluid

Connor M. Tierney
University of Mississippi. Sally McDonnell Barksdale Honors College

Visualization Techniques of Shear Wave Propagation in Wormlike Micellar Fluid

by
Connor Michael Tierney

A thesis submitted to the faculty of The University of Mississippi in partial fulfillment of the requirements of the Sally McDonnell Barksdale Honors College

Oxford, MS
May 2015

Approved by

_____
Advisor: Dr. Cecille Labuda

_____
Reader: Dr. Joel Mobley

_____
Reader: Dr. Joseph Gladden

ACKNOWLEDGEMENTS

I would like to extend my appreciation to Dr. Cecille Labuda for advising me throughout the entire research process. In addition to her unwavering patience and enthusiasm, she also provided insight into the proper employment of the scientific method, which was an invaluable supplement to my undergraduate education. I would also like to thank Dr. Joel Mobley and Dr. Joseph Gladden for taking the time to review my work. And finally, I am also appreciative of the opportunities and education that the Sally McDonnell Barksdale Honors College has provided me for the past four years.

ABSTRACT

In an aqueous solution amphiphilic molecules can self-aggregate and form a wormlike micellar fluid. These non-Newtonian fluids have been studied in the context of diagnostic medical imaging due to the fact that the fluids have viscoelastic properties and can act as a nonperishable model for human tissue. They also display flow-birefringence, which is a property that allows for the analysis of shear wave propagation through the fluid. However, one issue encountered at lower micelle concentrations is the inability to see the emergent birefringence pattern that results from shear wave propagation. In this study Experiment 1 was an analysis of shear wave propagation in a 500/300 mM CTAB/NaSal micellar fluid, which was seeded with microspheres, at 23° C. The results were compared to data obtained via birefringence pattern analysis in order to verify the legitimacy of using microspheres to study shear wave propagation in wormlike micellar fluids. It was found that there was an agreement between the shear wave speed obtained from the suspended microsphere analysis, which was 733 ± 25.5 mm/s, and the speed obtained from the birefringence pattern analysis, which was 722 ± 33 mm/s. This result is promising for analyzing shear wave propagation at lower micelle concentrations with suspended microspheres. In Experiment 2, shear waves of frequency varying from 50 Hz to 140 Hz were analyzed in order to determine whether the micellar fluid displayed dispersive properties. The results suggest that within this frequency range there is no substantial evidence suggesting that the fluid is dispersive. Further analysis with a higher resolution lens is suggested to investigate this further.

TABLE OF CONTENTS

LIST OF FIGURES

LIST OF SYMBOLS AND ABBREVIATIONS

CTAB - Cetyltrimethylammonium bromide

NaSal – Sodium salicylate

I – Intensity

θ – Relative angle

c – Velocity

ν – Frequency

λ – Wavelength

INTRODUCTION

Surfactants are amphiphilic molecules with a polar or charged hydrophilic "head" and a hydrophobic "tail" of carbon atoms. When placed into an aqueous solution at a concentration above a certain concentration known as the critical micelle concentration, amphiphilic molecules will self-aggregate to form micelles. The morphology of the micellar structures depends on the surfactant (Figure 1) concentration and solution temperature.[1]

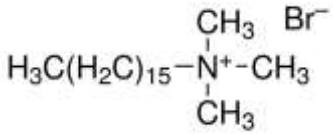

Figure 1: Cetyltrimethylammonium bromide (CTAB, $C_{19}H_{42}BrN$), the surfactant used (Image: Sigma-Aldrich online product catalog)

At low concentrations the most favorable energy state of the micelles is represented by a spherical conformation. In this conformation, the micelles spontaneously aggregate so that the hydrophobic "tails" are shielded from the aqueous solution with the hydrophilic "heads" forming the outer shell. At higher concentrations the most favorable conformation is tubular, or worm-like (Figure 2). The addition of a salt to the solution can stabilize longer tubular formations as the ions in solution mitigate the electrostatic repulsion between the hydrophilic heads.

The tubular micellar structures are several microns in length and have a diameter of about 15 nanometers.[2]

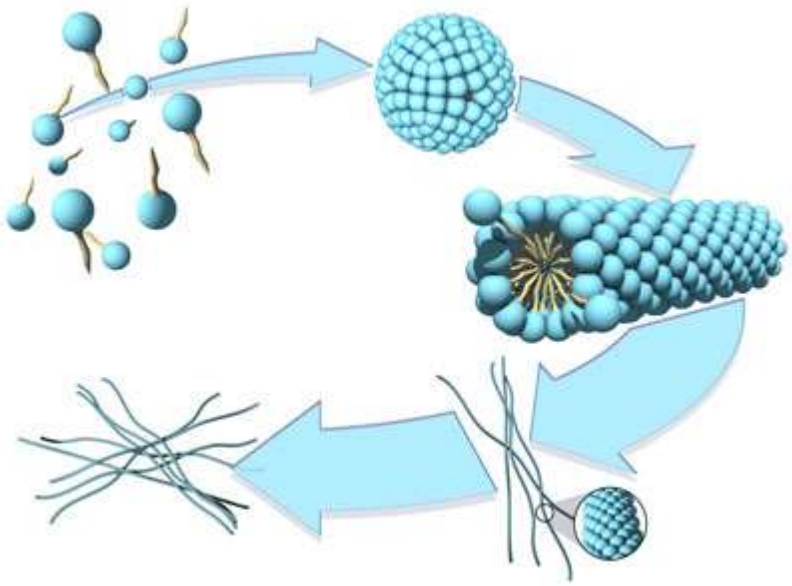

Figure 2: Conformations of micelles with increasing surfactant concentration (Image: Prof. Bjorn Lindman, University of Lund, Sweden)

The entanglement of the tubular structures is what gives the micellar fluid flow-birefringent and viscoelastic properties. A material is said to be birefringent if it displays more than one index of refraction.[3] Flow-birefringence is the emergence of birefringence when the fluid is sheared. In a relaxed state the worm-like tubules are isotropic and therefore optically inactive. When the fluid is sheared the tubules will untangle and align with the direction of the flow. Areas where the tubules are aligned will exhibit refractive index disparities relative to adjacent areas of aligned worms. The result is that the fluid will rotate polarized light and allow the emergence of birefringence pattern observed during shear wave propagation.[4] The

reason the pattern emerges in the presence of crossed polarizers can is described by Malus's Law[3]:

$$I(\theta) = I_0 \cos^2(\theta)$$

Without birefringence during shear wave propagation, the angle between the crossed polarizers is $\frac{\pi}{2}$ radians, which results in no transmission of the incident light through the container. However, once sheared, the fluid's ability to rotate the polarized incident light modifies the mathematical description seen above to the following:

$$I(\theta_i) = I_0 \cos^2(\theta_1) cos^2(\theta_2)$$

In the modified equation θ_1 represents the relative angle between the first polarizer and the direction of polarization of the sheared fluid at a given point, and θ_2 represents the angle between the direction of polarization of the sheared fluid at a given point and the second polarizer. Because the sheared fluid rotates the incident light, the light exiting the container is no longer polarized at an angle of $\frac{\pi}{2}$ radians relative to the second polarizer and the birefringence pattern becomes visible.

Worm-like micellar fluids also have the property of viscoelasticity, meaning that they exhibit both viscous and elastic properties under stress. The fluid is viscous because it resists deformation while stressed and is elastic because of its tendency to return to its original state after the source of stress is removed. The study of fluids with viscoelastic properties is important because of the potential for better understanding and improving shear wave elasticity imaging, which involves shear wave propagation through soft tissues via a focused beam of ultrasound. This process provides physicians with the ability to determine the elasticity of tissue

regions. The addition of elasticity data to ultrasonic or magnetic resonance images could help better differentiate between tissues and enhance the overall diagnostic process.[5] In addition to being viscoelastic like soft tissue, micellar fluids are also nonperishable, which makes them a practical benchtop model for understanding shear wave propagation in the context of diagnostic imaging.

In this work a micellar fluid was made with an aqueous solution of cetyltrimethylammonium bromide (CTAB, $C_{19}H_{42}BrN$) as the surfactant and sodium salicylate (NaSal, $C_7H_5NaO_3$) as the mitigating salt. Micellar fluids made with this particular surfactant-salt combination have been widely studied.[2,6,7] A study published in 2012 examined how shear wave propagation speed in a CTAB/NaSal micellar fluid is related to the concentration of the micelles. The results (Figure 3) indicate that there are distinct regimes of proportionality between shear wave speed and concentration of the micelles: the first concentration range showing a shear wave speed proportional to the square root of the concentration, and the second two concentration ranges showing a shear wave speed linearly proportional to the concentration but with different slopes.[2]

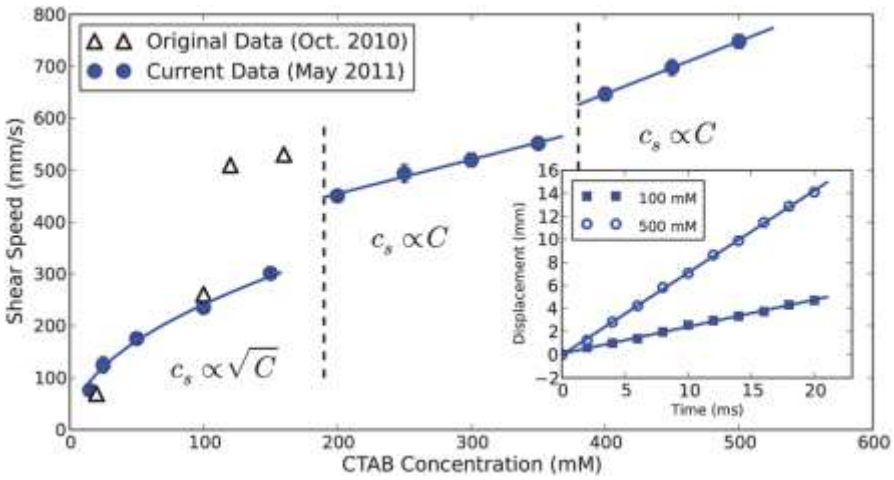

Figure 3: Results published by Gladden, Mobley, Skelton, and Gamble display shear wave speed as a function of micelle concentration

The distinct regimes of shear speed dependence on concentration are attributed to the changes in the micelles' morphology as the concentration increases. More generally, studies have shown that the size of the micellar structures increases with increasing concentration and decreases with increasing temperature.[7]

An issue that arises when measuring shear wave propagation via birefringence pattern analysis is that at lower micelle concentrations the birefringence pattern is relatively weak and more difficult to track and measure. By using micellar fluid seeded with microspheres the possibility arises of being able to measure shear waves regardless of the visibility of the birefringence pattern. In Experiment 1, this type of analysis was carried out. In Experiment 2 the micellar fluid was tested to see if it displayed dispersive properties. For both experiments a CTAB/NaSal micellar fluid solution with a 500 mM surfactant concentration was used at a temperature of about 23° C.

MATERIALS AND METHODS

Preparation of the Micellar Fluid

The micellar fluid, with a 5:3 surfactant to salt ratio, was prepared using cetyltrimethylammonium bromide (CTAB, $C_{19}H_{42}BrN$) and sodium salicylate (NaSal, $C_7H_5NaO_3$) (Sigma-Aldrich, St. Louis, MO). In order to prepare a 1500 mL volume of a 500 mM solution, 1500 mL of HPLC grade water (Fisher Scientific, Waltham, MA) was heated to a temperature between 70 and 90° C. When the water reached the proper temperature, 273.338 g of CTAB and 72.045 g of NaSal were added to separate beakers, each containing a portion of the water, and the mixture was stirred with a magnetic stirrer for 2 hours. After each mixture was fully dissolved, the NaSal solution was added to the CTAB solution and the combined mixture was covered and mixed on a magnetic stirrer hotplate at a temperature of 80° C for about 24 hours.

A 320 mL sample of the 500 mM micellar fluid was poured out and heated to reduce viscosity, thus facilitating the mixing of particles into the fluid. Once heated, polyethylene microspheres of diameter 212-250 μm and density 0.995 g/cm^3 (Cospheric, Santa Barbara, CA) were added to the fluid while it was continuously stirred with a magnetic stirring rod until the microspheres were evenly dispersed throughout (Figure 4). While still hot, the sample was then transferred to an acrylic container with a 2 inch x 2 inch square cross-section and a height of 6 inches. Heating tape (36001-54, Cole-Parmer, Vernon Hills, IL) was then wrapped around

the container to heat the fluid and reduce the viscosity, which facilitated the escape of trapped gas bubbles.

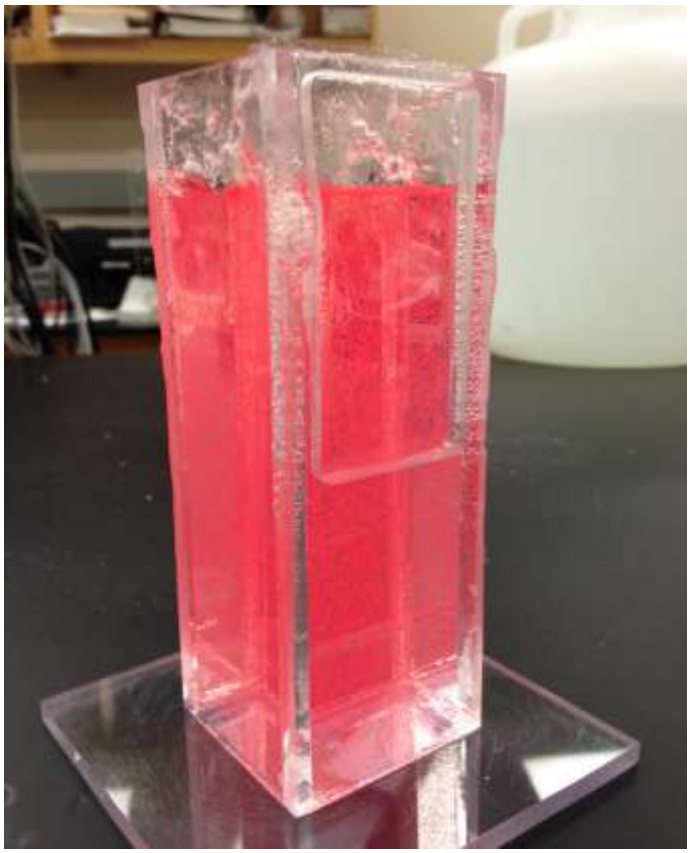

Figure 4: Photograph of micellar fluid with microspheres

Experimental Setup

A halogen lamp with a diffuser was used to backlight the fluid. A high-speed camera (Edgertronic, Sanstreak Corp., San Jose, CA) with a 105 mm lens (Nikon, Melville, NY) was used to capture videos of the propagation of the shear waves through the fluid. The mechanical wave driver (SF-9324, Pasco Scientific, Roseville, CA) was fitted with a 1 inch x 1 inch acrylic plate, which was attached to an L-shaped

rod and lowered until it touched the surface of the fluid. Shear waves were produced by driving the wave driver with a sinusoidal signal from a function generator (395, Wavetek, Austin, TX). A schematic diagram and photographs of the experimental setup and the micellar fluid with microspheres are shown below in Figures 5 and 6.

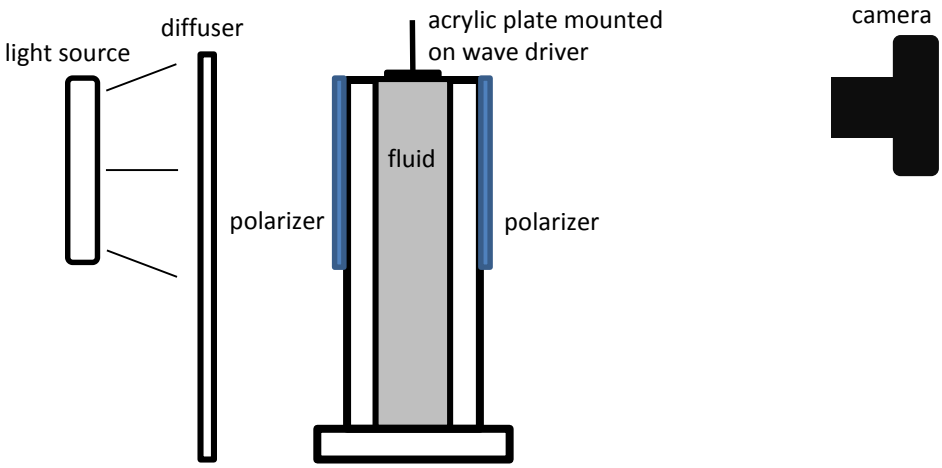

Figure 5: Schematic diagram of experimental setup

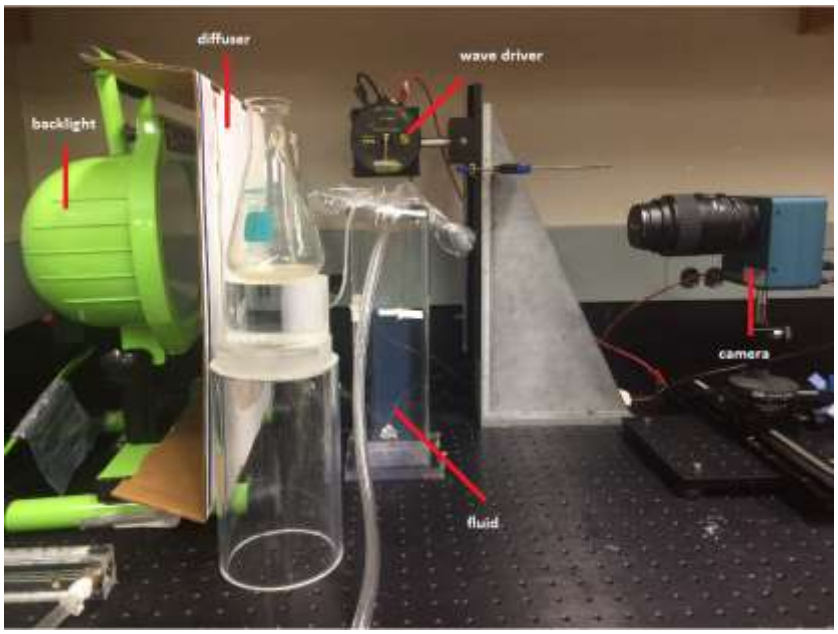

Figure 6: Photograph of experimental setup

EXPERIMENT 1: VISUALIZATION OF SHEAR WAVES IN A MICELLAR FLUID USING MICROSPHERES

Introduction

Experiment 1 involves comparing the shear wave speed determined by tracking oscillating suspended microspheres with the speed determined using the analysis of the time-dependent birefringence pattern. This was carried out in order to verify the legitimacy of using suspended microspheres as a means of determining shear wave speeds. There is also an analysis of wave amplitude as a function of depth and horizontal position using the data obtained while tracking the motion of the microspheres.

Methods

Experimental Setup

For Experiment 1, two types of videos were recorded. The first type of video used unpolarized backlighting to observe the motion of the microspheres, and we will refer to this as the unpolarized video. The second type of video used polarizers to observe the motion of the microspheres and the accompanying birefringence pattern simultaneously. We will refer to this as the polarized video.

As described, the unpolarized video was recorded by backlighting the microsphere-seeded fluid with unpolarized light. The video obtained shows the

motion of the microsphere particles as a response to the propagating shear wave. The polarized videos was recorded by placing a polarizer between the backlight and the fluid and another crossed polarizer on the other side of the fluid (Figure 5). Shear waves were generated in the microsphere-seeded fluid, and in the case of the unpolarized video the motion of the microspheres was captured. In the polarized video, the addition of the polarizers allowed the birefringence pattern to become visible, and in this video the birefringence pattern and the microsphere motion were recorded simultaneously. For both visualization techniques a wave frequency of 61 Hz was used. The videos were captured at 61 Hz instead of 60 Hz in order to prevent stroboscopic phenomena from the halogen lamp running on a 60 Hz alternating current. In both videos a ruler was mounted along the side of the fluid container in order to determine a scale factor.

Wavelength and Shear Wave Speed Determination by Birefringence Pattern

In order to verify the microsphere visualization technique with the birefringence pattern technique used in an earlier study[2], the shear wave speeds were obtained by experimentally determining the wavelengths of the shear wave and multiplying the wavelengths by the frequency:

$$c = \nu\lambda$$

In order to determine the wavelength from the birefringence pattern, the captured video was first imported into MATLAB (Mathworks, Natick, MA) statistical analysis software. A sequence of frames was then extracted from the video and the contrast was adjusted in order to make the birefringence pattern more visible.

From here the distance in pixels between the top and bottom edges of a single fringe were measured in order to determine the coordinates of the center of the fringe. This same process was carried out for the third fringe relative to the first. The combination of these two measurements yielded the distance in pixels between the first and third fringe, which is representative of the wavelength. This distance was multiplied by the scale factor of 0.03703 mm/pixel to yield the actual value of the wavelength in millimeters. The scale factor was determined by calculating a pixel-to-length ratio using a still frame of a millimeter scale that was in the same focal plane as the propagating waves that were captured.

Wavelength and Shear Wave Speed Determination by Particle Motion

In order to determine the wavelength from the motion of the microspheres, the videos were imported into ImageJ[8] and the grayscale range was inverted in order to allow the tracking of the particles. With the combination of MosaicSuite and ImageJ software, 100 frames of video were analyzed to track the motion of about 2000 microspheres (Figures 7(a) and 7(b)).

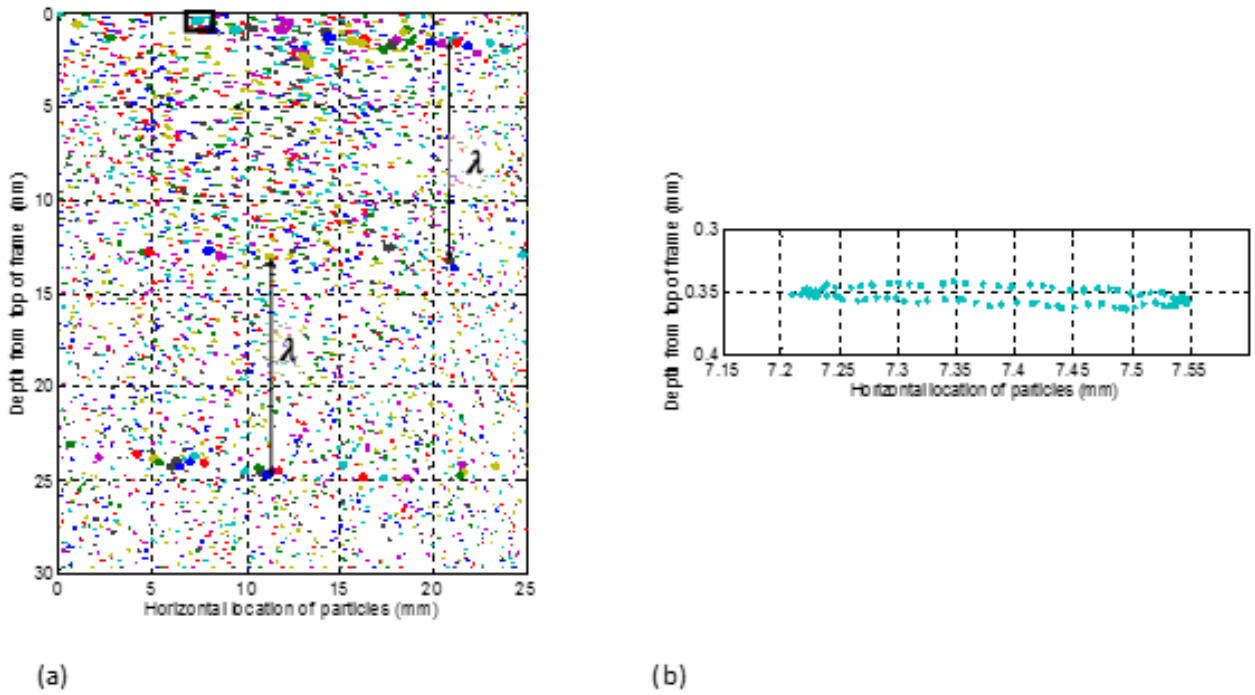

Figures 7(a) & 7(b): The collection of tracked trajectories with a typical microsphere path plot

The horizontal positions of the microspheres were then plotted as a function of time (Figure 8(c)). Particles that were in phase with one another were identified by determining which particles reached their maximum horizontal displacement at coinciding times. The vertical distance between the in-phase particles was measured to determine the wavelength in pixels. This length was converted to millimeters using the scale factor of $0.03846\ \mathrm{mm/pixel}$, which was recalculated for the new set of videos. The wavelength was determined in this manner for 19 pairs of vertically separated in-phase particles. The mean and standard deviation for both the wavelength and the shear wave speed were then determined.

Dependence of particle amplitude on location

Using the tracking data obtained for the particles the amplitudes of oscillation were measured as a function of both vertical depth and horizontal position. In order to determine how the particles' amplitudes varied with depth, the particles were selected in 2x2 mm squares with the criterion that at least 8 particles must be present in each square. Within each chosen square the average amplitude and depth of the particles was determined along with the standard deviation. To determine how the particles' amplitudes varied relative to horizontal location, the vertical location of a 2x2 mm square was fixed at 1 mm below the top of the frame and the horizontal location was varied across the width of the frame. The average amplitudes relative to their respective horizontal locations were then calculated along with the standard deviation. The plots are shown in Figures 9 and 10 respectively.

Results

The average wavelength that was determined from the analysis of in-phase microspheres was 12.0 mm with a standard deviation of 0.42 mm. This corresponds to a shear wave speed of 733 ± 25.5 mm/s, which is consistent with a speed of 750 mm/s measured in a previously cited work involving micellar fluid of the same concentration and composition.[2]

The wavelength that was determined from the analysis of the birefringence pattern was 11.5 mm with a standard deviation of 0.55 mm. This corresponds to a shear wave speed of 722 ± 33 mm/s, which is consistent with both the speed

determined by analyzing the microspheres and the speed reported in the work mentioned previously.

Qualitatively, a full displacement cycle corresponded to the passing of three consecutive fringes through the location of a particle. At zero displacement, the particle was aligned with the center of the birefringent fringe passing through its vertical location. At maximum displacement, both negative and positive, the particle was aligned with the birefringent fringe boundary. This is illustrated in Figures 8(a) and 8(b) with a displacement plot in Figure 8(c).

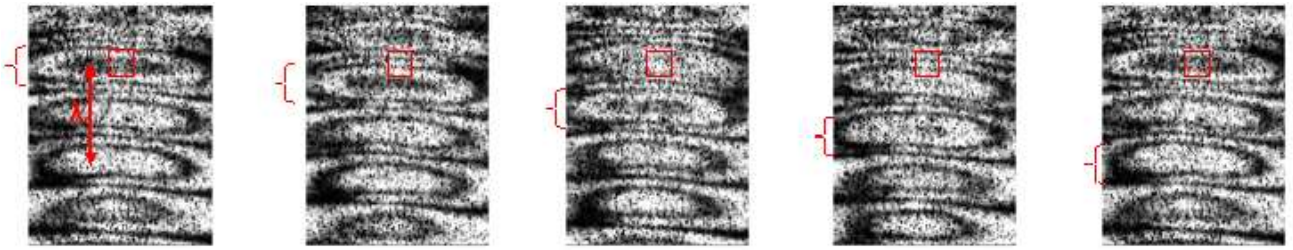

Figure 8(a): Microsphere location (in boxes) relative to a fringe labeled with a bracket

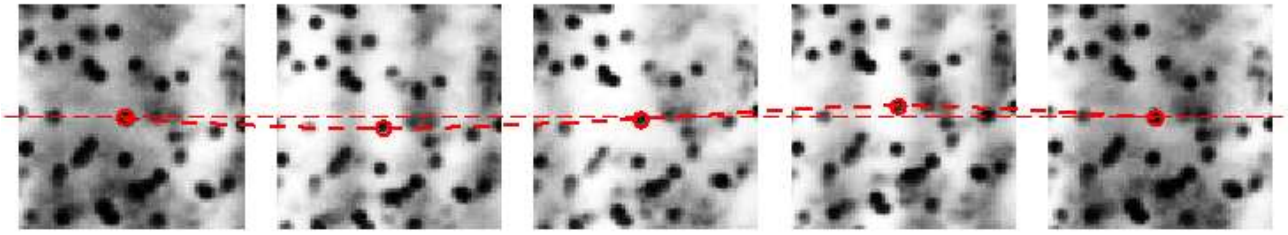

Figure 8(b): Enlarged and rotated view of the boxes in Figure 8(a)

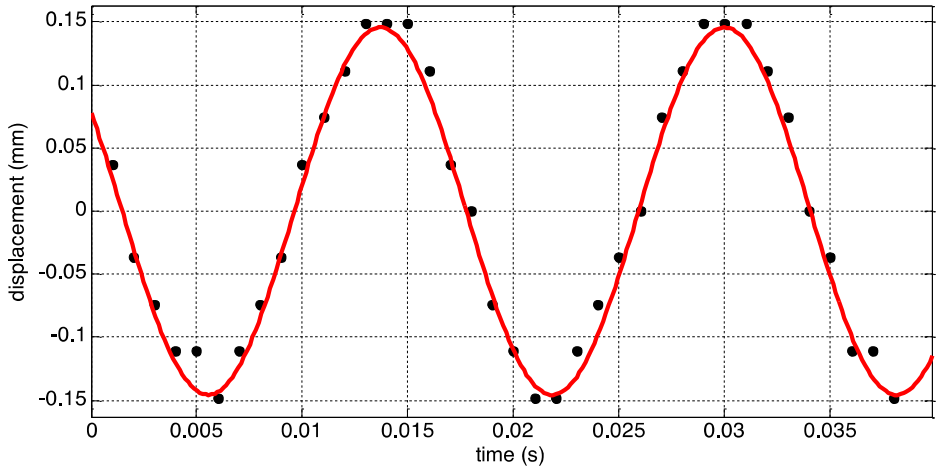

Figure 8(c): Microsphere displacement plot

In Figure 8(c) the dots represent measured values for microsphere displacement perpendicular to the direction of the propagating shear wave and the red curve is the sinusoidal fit with $d = 0.1456\sin(385.6t - 3.707)$, where d is the microsphere displacement in millimeters from equilibrium and t is time in seconds. The R-square value for the plot is 0.9842 and the frequency yielded is 61.4 Hz. Both the waveform and the yielded frequency are consistent with the 61 Hz sinusoidal wave generated to produce the shear wave.

The maximum displacement of the microspheres also varied with their depth and horizontal location. Figure 9 shows the plot for the average particle amplitude over a 2 mm range as a function of depth. The plot also includes an error bar of two standard deviations, which is representative of the variation from the mean and the general distribution of average particle amplitudes over a 2 mm range.

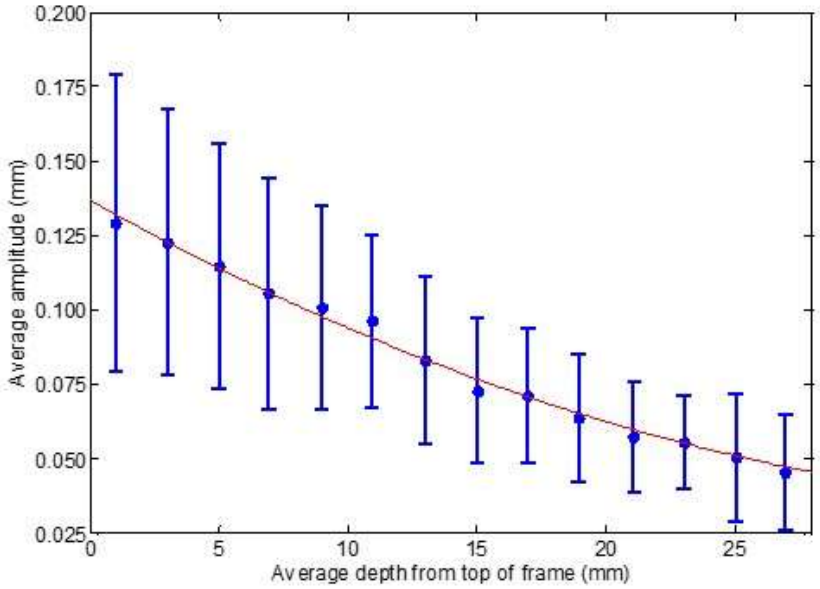

Figure 9: Variation of microsphere amplitude with depth for particles in a 2x2 mm area in the horizontal center of frame

The quadratic fit shown in Figure 9 is $A = 0.00011y^2 - 0.0097y + 0.27$, where A is the average amplitude and y is the vertical distance from the top of the frame. As expected, the average maximum displacement from equilibrium decreases as the distance from the wave source increases.

Figure 10 shows the average particle amplitude over a 2 mm range as a function of horizontal location. As in the previous plot, Figure 10 also includes a two standard deviation error bar.

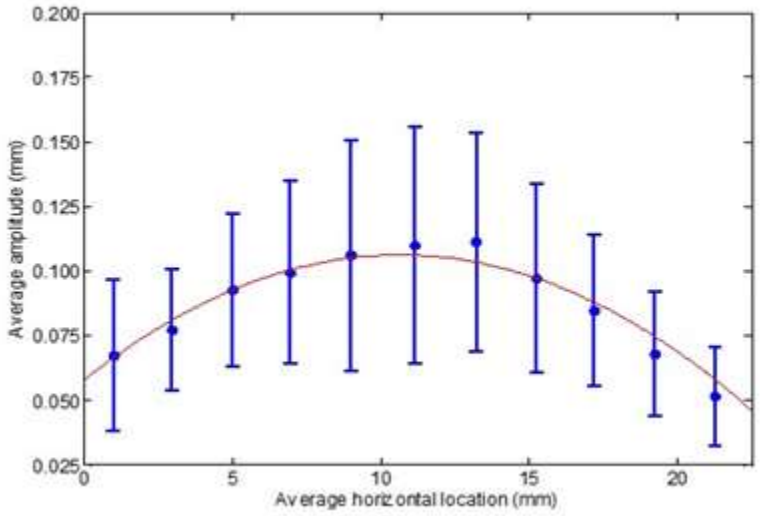

Figure 10: Variation of microsphere amplitude with horizontal position for particles in a 2x2 mm area

The quadratic fit shown in Figure 10 is $A = -0.00086x^2 + 0.018x + 0.012$, where A is the average amplitude and x is the horizontal distance from the right edge of the frame. As expected, the average maximum displacement from equilibrium increases as the distance from the container walls increases.

Discussion and Conclusion

The wavelength and the speed of the shear wave are in agreement for the microsphere tracking technique and the birefringence pattern tracking technique. Furthermore, they are also consistent with shear wave speeds measured in a previous work.[2] Using the polarized videos it was found that the microsphere displacements were at equilibrium at the center of the birefringence fringes and the displacements were at a maximum at the birefringence fringe boundaries. The data gathered from the tracking of the microspheres show that the amplitude of the shear wave is inversely proportional to the square of the depth.

Because microspheres can be uniformly distributed within micellar fluids in a wide range of concentrations, this technique offers the possibility of determining shear wave attenuation when the micelle concentration is low and the emergent birefringence pattern is relatively weak and difficult to analyze. It is also a promising visualization technique because it allows one to circumvent the issue of ensuring that the micellar fluid is uniformly lit by the backlight, as failure to do so will result in artifactual intensity variations in the birefringence pattern.

EXPERIMENT 2: SPEED OF SHEAR WAVES AS A FUNCTION OF FREQUENCY IN WORMLIKE MICELLAR FLUID

Introduction

The purpose of Experiment 2 was to determine whether the CTAB/NaSal micellar fluid displays dispersive properties. Dispersion is a property where wave speed will vary depending on the frequency of the propagating waves. A familiar phenomenon involving frequency dispersion is the propagation of white light through a prism. When white light interfaces with a translucent prism the speed of the light will vary according to the index of refraction. Because the index of refraction varies with the frequency of the light, the result is the speed of the light waves depending on their frequencies. Because the frequency of the wave driver producing the shear waves in the micellar fluid is a constant value that is input by the experimenter, the changes in the speed of the shear waves can be determined by measuring their wavelengths at different frequencies.

Methods

For Experiment 2 sinusoidal waves of frequency ranging from 50 Hz to 140 Hz were generated using the function generator. The frequencies were generated in 10 Hertz increments, except for one measurement, which was taken at 61 Hz. The speed of the shear waves at each frequency was determined by measuring the

wavelengths in the same manner as discussed in the *Wavelength and Shear Wave Speed Determination by Birefringence Pattern* section of Experiment 1.

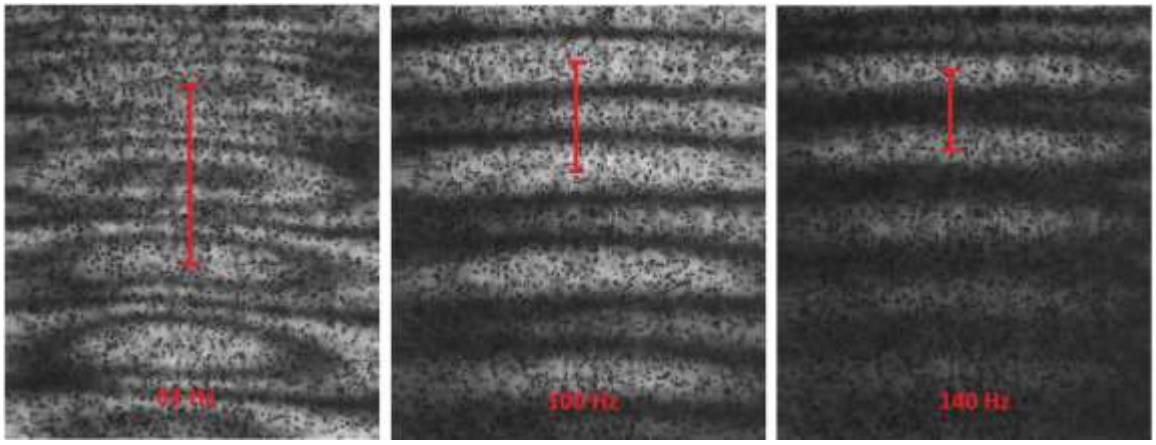

Figure 11: Frame captures of birefringence pattern with wavelengths labeled at frequencies of 61 Hz, 100 Hz, and 140 Hz respectively

The measured wavelengths were then multiplied by the frequency of the shear wave in order to yield the value for the wave speed. The measured shear wave speeds at each frequency are shown in Table 1 with a plot of the results in shown in Figure 12.

Results

One can see from Table 1 that there was no significant variation in the shear wave speeds relative to frequency.

Table 1: Measured shear wave speeds and wavelengths at varying frequencies

Frequency (Hz)	Wavelength (mm)	Speed (mm/s)	Standard deviation
50	14.9	747	$\pm$ 5
61	12.4	754	$\pm$ 12
70	10.7	752	$\pm$ 8
80	9.33	746	$\pm$ 16
90	8.32	749	$\pm$ 6
100	7.46	746	$\pm$ 6
110	6.82	750	$\pm$ 15
120	6.19	743	$\pm$ 8
130	5.83	758	$\pm$ 20
140	5.38	753	$\pm$ 17

The plot seen in Figure 12 includes a red linear fit line and each data point (blue) includes a two standard deviation error bar.

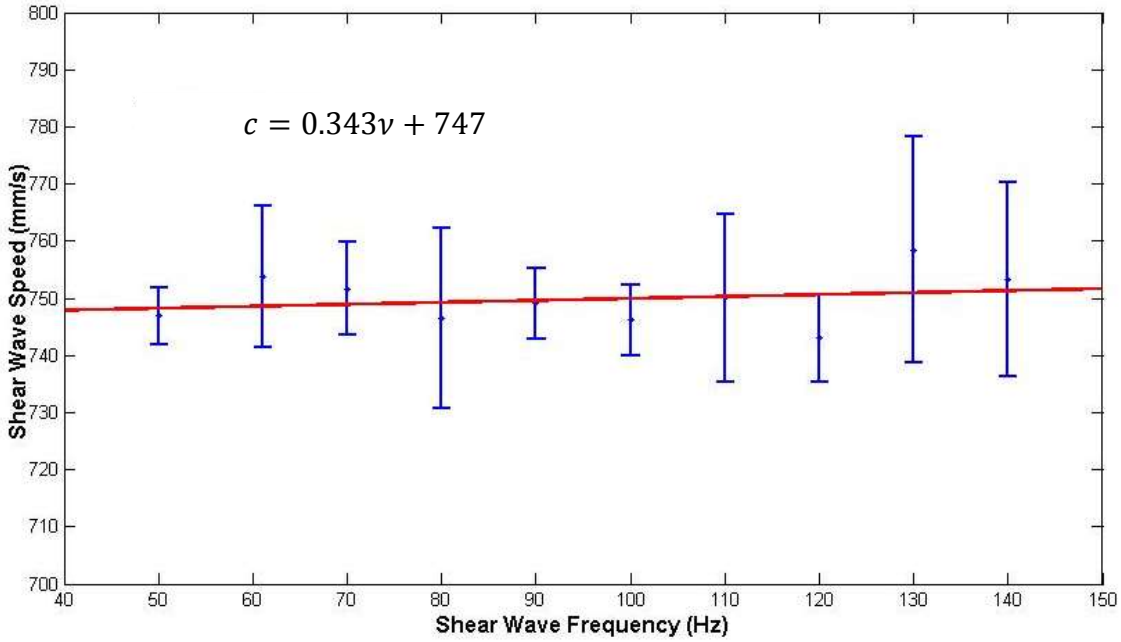

Figure 12: Shear wave speed as a function of frequency

Discussion and Conclusion

In the frequency interval from 50 Hz to 140 Hz there is no significant variation of shear speed as a function of frequency, indicating that CTAB/NaSal micellar fluid at a 500 mM surfactant concentration displays no dispersive properties. In order to further support or refute this claim it is recommended that the analysis be done over a wider interval of shear wave frequencies. It should be noted that the birefringence pattern produced is more difficult to analyze at lower frequencies ($0\ Hz\ \leq \nu \leq 40\ Hz$) due to the fact that the wavelengths are very large relative to the captured frames. It is also progressively more difficult to analyze the

shear wave at higher frequencies ($\nu > 150\ Hz$) due to the fact that the birefringence pattern has a shorter wavelength. The short wavelengths make it difficult to differentiate between adjacent fringes. By employing the method involving the tracking of suspended microspheres one could potentially alleviate this issue. However, because particle amplitude is lower at higher frequencies, a higher resolution lens must be used in order to observe the motion of microspheres across relatively small distances.

FINAL CONCLUSIONS

In summary, Experiment 1 showed that the utilization of microspheres in conjunction with particle tracking software can be an effective means of determining shear wave speed at a wide range of surfactant concentrations. This visualization technique also seems promising in that it could allow further exploration of shear speed attenuation. Both of these possibilities could prove to be useful for furthering the development of shear wave elasticity imaging, which can add a tissue elasticity map to ultrasonic images and improve the ability to differentiate between tissues. The microsphere visualization technique also confirms that shear wave amplitude is indirectly proportional to the distance from the wave driver and also directly proportional to the distance from the fluid container boundaries. In Experiment 2 it was found that in a frequency range from 50 to 140 Hz there is no evidence that CTAB/NaSal micellar fluid with a surfactant concentration of 500 mM displays dispersive properties. It is suggested that a larger concentration range is explored using the particle tracking visualization technique with a higher resolution lens in order to investigate this further.

REFERENCES

1. J. Rothstein. “Strong flows of viscoelastic wormlike micelle solutions,” Rheol. Rev. 2009, 1–46 (2008).
2. J.R. Gladden, A.M. Gamble, C.E. Skelton, and J. Mobley. “Shear waves in viscoelastic wormlike micellar fluids over a broad concentration rang*e*,” *Journal of the Acoustical Society of America,* 131, no. 3, (2012): 2063-2067.
3. E. Hecht. 2002. *Optics – 4th Edition.* San Francisco (CA): Addison Wesley.
4. B.H. Cipriano, D. Danino, B.D. Frounfelker, G.C.Kalur. “Persistence of Birefringence in Sheared Solutions of Wormlike Micellar Fluids,” *Langmuir*, 2009, 25 (1), 167-172.
5. A.P. Sarvazyan, O.V. Rudenko, S.D. Swanson, J.B. Fowlkes, and S.Y. Emalianov. “Shear wave elasticity imaging: A new ultrasonic technology of medical diagnostics,” Ultrasound Med. Biol. 24 (1998).
6. V. Lutz-Bueno, J. Kohlbrecher, P. Fischer. “Shear thickening, temporal shear oscillations, and degradation of dilute equimolar CTAB/NaSal wormlike solutions,” Rheologica Acta, 2013, 52 (4), 297-312.
7. N.C. Das, H. Cao, H. Kaiser, G.T. Warren, J.R. Gladden, P.E. Sokol. “Shape and size of highly concentrated micelles in CTAB/NaSal solutions by small angle neutron scattering,” *Langmuir,* 2012, 28 (33), 11962-11968.
8. ImageJ (W.S. Rasband, U. S. National Institutes of Health, (1997-2014), http://imagej.nih.gov/ij/

APPENDIX A

agilenttest.m

```
clear all;
wavetek395GPIBID=9;
hpagilentGPIBID=10;
funcgenGPIBID=wavetek395GPIBID;
funcgen=gpib('ni', 0, funcgenGPIBID);

fopen(funcgen);
fprintf(funcgen,'FUNC SIN');
fprintf(funcgen,'FREQ 60');
fprintf(funcgen,'VOLT 1.5');

pause(0.1);
fprintf(funcgen,'OUTP ON');
pause(2.5);
fprintf(funcgen,'OUTP OFF')

fclose(funcgen)
disp('end test Wavetek');
```

APPENDIX B

readvideo.m

```
clear all;
close all;
filename='slomo_1406208015_22.4degrees.mov';
[pathstr,name,ext] = fileparts(filename);
micellar = VideoReader(filename);
fprintf('Reading video file.');
video = read(micellar,'native');

nFrames = micellar.NumberOfFrames;
vidHeight = micellar.Height;
vidWidth = micellar.Width;

mov(1:nFrames) = ...
   struct('cdata',zeros(vidHeight,vidWidth, 3,'uint8'),...
        'colormap',[]);

for k = 1 : nFrames
   mov(k).cdata = read(micellar,k);
end


for i=100:1:125
   h(i)=figure;
   [im,map] = frame2im(mov(i));
   J=rgb2gray(im);
   K=J;
   imshow(K);

   axis equal;
   axis tight;
end
```

APPENDIX C

createfit.m

```
[xData, yData] = prepareCurveData( xmanualplot, ymanualplotmm );

ft = fittype( 'fourier1' );
opts = fitoptions( 'Method', 'NonlinearLeastSquares' );
opts.Display = 'Off';
opts.StartPoint = [0 0 0 0.425978664893531];

[fitresult, gof] = fit( xData, yData, ft, opts );

figure( 'Name', 'untitled fit 1' );
h = plot( fitresult, xData, yData );
legend( h, 'ymanualplotmm vs. xmanualplot', 'untitled fit 1', 'Location', 'NorthEast' );

xlabel( 'xmanualplot' );
ylabel( 'ymanualplotmm' );
grid on
```

APPENDIX D

lambdacalc.m

```
plr=0.0391;
freq=61;
a1=[5 10 15 13 17 22 19 19 22 12];
a2=[106 111 120 108 117 127 112 119 122 106];
a3=[217 224 229 223 229 234 228 230 235 222];
a4=[315 321 328 321 327 330 322 329 331 316];
lamb=[ ];
lambcs=[ ];
for i=1:10
   c1=(a3(i)+((a4(i)-a3(i))/2))-(a1(i)+((a2(i)-a1(i))/2));
   lamb(i)=c1;
   lambcs(i)=c1*plr*freq;
end
lambda=mean(lamb);
cs=lambda*plr*freq;
SD=std(lambcs);
```